ARTICLES
https://doi.org/10.1038/s41551-018-0192-3
nature biomedical engineering

Treatment of chronic pain by designer cells controlled by spearmint aromatherapy

Hui Wang[1], Mingqi Xie[1], Ghislaine Charpin-El Hamri[2], Haifeng Ye[3] and Martin Fussenegger[1,4]*

Current treatment options for chronic pain are often associated with dose-limiting toxicities, or lead to drug tolerance or addiction. Here, we describe a pain management strategy, based on cell-engineering principles and inspired by synthetic biology, consisting of microencapsulated human designer cells that produce huwentoxin-IV (a safe and potent analgesic peptide that selectively inhibits the pain-triggering voltage-gated sodium channel $Na_V1.7$) in response to volatile spearmint aroma and in a dose-dependent manner. Spearmint sensitivity was achieved by ectopic expression of the R-carvone-responsive olfactory receptor OR1A1 rewired via an artificial G-protein deflector to induce the expression of a secretion-engineered and stabilized huwentoxin-IV variant. In a model of chronic inflammatory and neuropathic pain, mice bearing the designer cells showed reduced pain-associated behaviour on oral intake or inhalation-based intake of spearmint essential oil, and absence of cardiovascular, immunogenic and behavioural side effects. Our proof-of-principle findings indicate that therapies based on engineered cells can achieve robust, tunable and on-demand analgesia for the long-term management of chronic pain.

Chronic pain is one of the most difficult medical conditions to manage, affecting more than 10% of the world's population[1,2]. In particular, treatment options for persistent peripheral pain resulting from chronic inflammation (nociceptive pain) or nerve damage (neuropathic pain) owing to cancer, infectious diseases, physical injuries or diabetes are limited[3,4]. For example, non-steroidal anti-inflammatories have dose-limiting side effects, whereas morphine involves the risk of addiction or tolerance[2,5]. Although the venom-derived ω-conotoxin peptide ziconotide (SNX-111; also known as Prialt) circumvents these issues and has been licensed for the treatment of severe chronic pain, the only effective administration route is intrathecal injection, which poses high risks[6,7]. Therefore, there is still an urgent need for safe and effective pain treatment strategies.

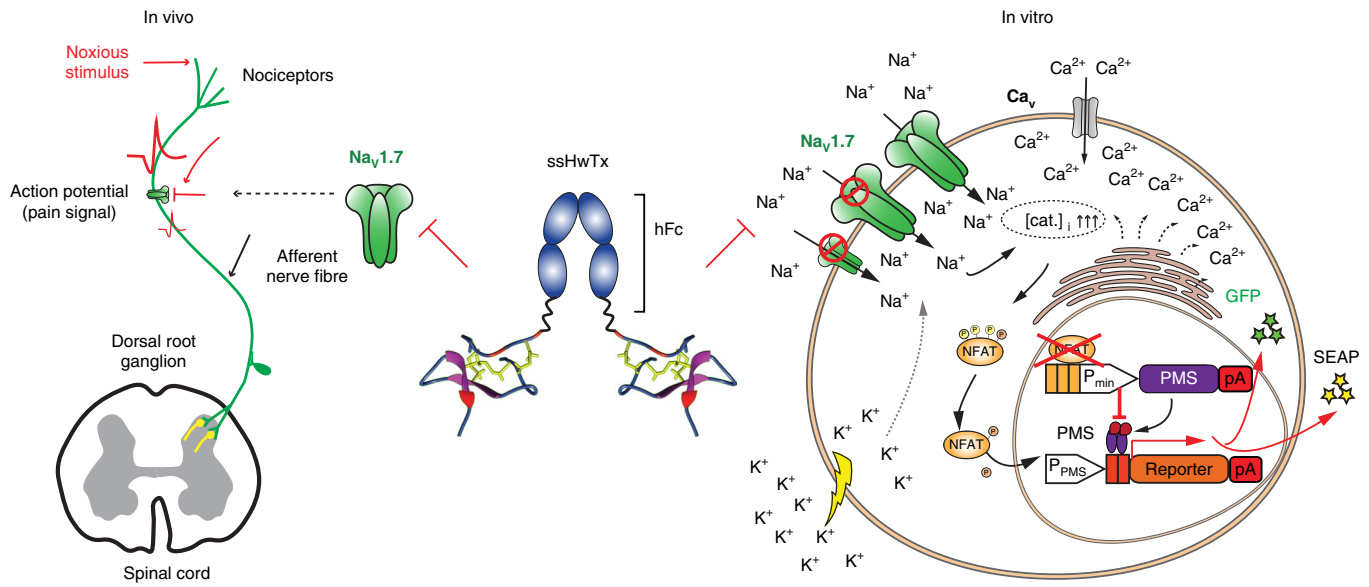

Fig. 1 | Engineering of ssHwTx. Principle of PainAssay. In humans, $Na_V1.7$ coordinates the transmission of pain signals along peripheral neurons. Inhibition of $Na_V1.7$ results in suppression of pain perception. In a $Na_V1.7$-specific PainAssay in vitro (see Supplementary Fig. 1a), membrane depolarization triggers cytosolic calcium increase and P_{NFAT}-driven transsilencing of reporter gene expression. Inhibition of $Na_V1.7$ by analgesic compounds such as ssHwTx (hFc-HwTx-IV) antagonizes depolarization-mediated gene silencing and activates reporter gene expression. PMS denotes mammalian paraben-mediated transsilencer[45]. [cat.] denotes intracellular cation levels. P_{min} denotes minimal promoter. pA denotes polyadenylation signal. Ca_V denotes voltage-gated calcium channels. The circled P denotes a phosphorylated protein residue.

[1]Department of Biosystems Science and Engineering, ETH Zurich, Basel, Switzerland. [2]Département Génie Biologique, Institut Universitaire de Technologie, IUT, Villeurbanne, France. [3]Shanghai Key Laboratory of Regulatory Biology, Institute of Biomedical Sciences and School of Life Sciences, East China Normal University, Shanghai, China. [4]Faculty of Science, University of Basel, Basel, Switzerland. *e-mail: fussenegger@bsse.ethz.ch

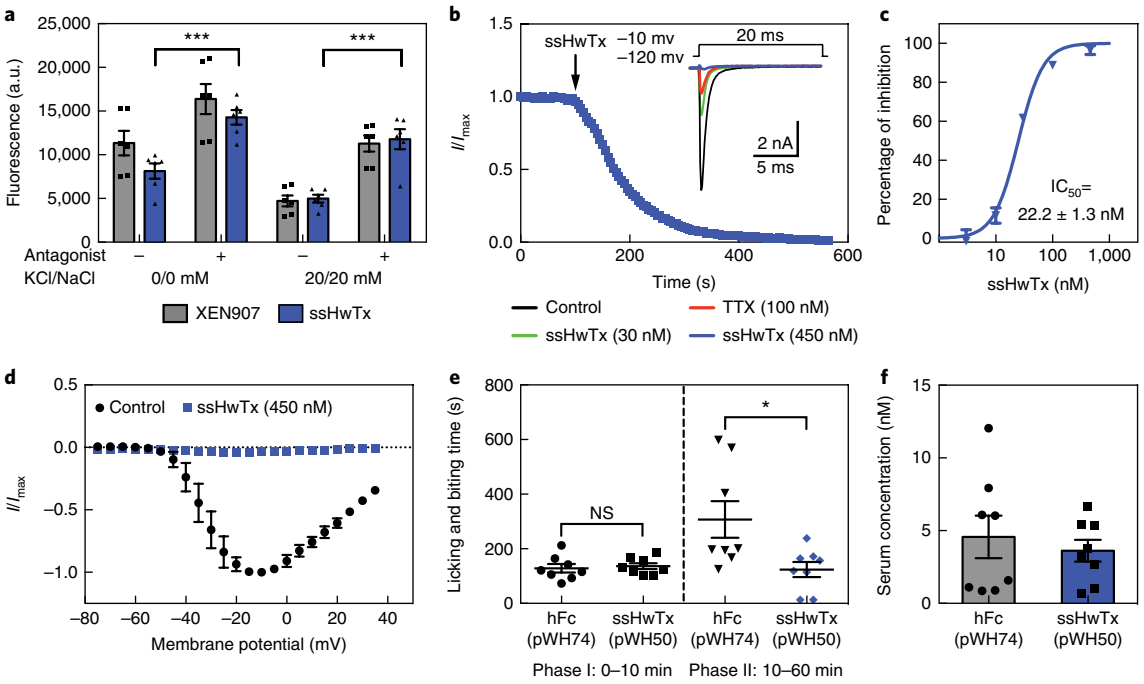

Fig. 2 | Engineering and validation of ssHwTx. a, GFP-based PainAssay. HEK293 cells were cotransfected with pWH68 (P_{PMS}-TurboGFP-pA), pMX109 (P_{NFAT3}-PMS-pA) and pNaEx8 (P_{hCMV}-hNa_V1.7-pA), and cultured for 24 h in XEN907-enriched (5 µM) or ssHwTx-enriched medium (450 nM) containing different concentrations of potassium chloride (KCl) and sodium chloride (NaCl), then transferred into fresh culture medium containing the same amount of chemicals (5 µM) or ssHwTx (450 nM) and cultivated for another 24 h. GFP levels were scored at 48 h after first exposure to Na_V1.7-specific inhibitors. Data are mean ± s.e.m., $n = 6$ independent experiments. 0/0 mM and 20/20 mM denotes KCl/NaCl-concentrations (in mM) added to the culture medium, in particular 0mM of both or 20mM of both, either in the presence (+) or absence (–) of XEN907 or ssHwTx. **b**–**d**, Patch clamp experiments showing the effects of ssHwTx on inward current kinetics (**b**) and dose-dependent (**c**) or voltage-dependent (**d**) hNa_V1.7 inhibition. **b**, Current amplitudes generated by a 20 ms, –10 mV depolarizing potential from a holding potential of –120 mV at 0.2 Hz in the presence of 450 nM ssHwTx. Inset shows representative current trajectories inhibited by 450 nM ssHwTx or 100 nM tetrodotoxin (TTX, positive control). **c**, ssHwTx dose-dependent inhibition of hNa_V1.7 stably expressed in CHO-K1 cells. **d**, hNa_V1.7 current–voltage relationships in the presence or absence of 450 nM ssHwTx generated using 50 ms depolarization steps between –80 mV and –40 mV in 5 mV increments from a holding potential of –120 mV. All data (**b**–**d**) were normalized to the maximum current amplitude (I/I_{max}) and presented as mean ± s.d., $n = 3$ independent cells. **e**, Validation of ssHwTx analgesic potency in mice with the formalin test; 10×10^6 microencapsulated HEK293 cells transgenic for constitutive ssHwTx secretion (pWH50; human cytomegalovirus immediate early promoter-driven ssHwTx-Pa (P_{hCMV}-ssHwTx-pA)) or negative control cells consisting of pWH74-transgenic HEK293 (pWH74; P_{hCMV}-hFc-pA) were implanted into mice. Using the formalin-induced persistent pain model, pain behaviour during the acute phase (phase I: 0–10 min after intraplantar formalin injection) and chronic phase (phase II: 10–60 min) was analysed by scoring total licking and biting times of the formalin-injected paw at 48 h after implantation. **f**, Production of ssHwTx in vivo. Therapeutic transgene product levels in the bloodstream were quantified using a human Fc-specific enzyme-linked immunosorbent assay after completion of the formalin test described in **e**. Data in **e**,**f** are shown as the mean ± s.e.m. and symbols indicate individual data points, statistics by two-tailed *t*-test, $n = 8$ mice per group. $^*P < 0.05$ versus control; NS, not significant. a.u., arbitrary units. All plasmids are described in Supplementary Table 1.

Huwentoxin-IV (HwTx-IV), also known as mutheraphotoxin-Hh2a, is a natural analgesic peptide isolated from the Chinese bird spider *Haplopelma schmidti*. HwTx-IV is a selective inhibitor of the voltage-gated sodium channel Na_V1.7, which is the prime molecular target for treatment of pain[4]. HwTx-IV inhibits human Na_V1.7 (hNa_V1.7) with high specificity (half-maximum inhibitory concentration $IC_{50} \approx 0.4$ nM)[8], while showing low affinity for other sodium channel isoforms hNa_V1.4 ($IC_{50} \approx 3.9$ µM) and hNa_V1.5 ($IC_{50} \approx 25$ µM)[8,9]; this is crucial to prevent adverse effects on skeletal and cardiac muscles[9]. Indeed, preclinical studies of peripherally administered HwTx-IV confirmed that it can suppress both nociceptive and neuropathic pain syndromes in mice[10]. However, because of low bioavailability, repeated injections at high doses are required to relieve pain.

In this work, we aimed to develop a next-generation pain management strategy. For this purpose, we first developed a stabilized HwTx-IV variant custom-designed for high-level production and secretion in human cells (secretion-engineered and stabilized HwTx-IV (ssHwTx)). Then, to achieve production and secretion of ssHwTx under remote control by spearmint aromatherapy, we designed AromaCell, a human embryonic kidney cell line (Hana3A) stably transgenic for the spearmint aroma R-carvone-stimulated ssHwTx expression. We considered that this approach would have the potential to provide robust, tunable and on-demand analgesia for long-term management of chronic pain while also enabling patient-selected drug termination to prevent the development of drug tolerance or addiction[3].

Results

Design and validation of ssHwTx. To increase the plasma half-life and production efficiency of HwTx-IV, we modified the molecule by fusing a human immunoglobulin-G1 fragment crystallizable (Fc) domain containing a human interleukin-2 derived secretion signal[11] to the N terminus of HwTx-IV, resulting in a stabilized HwTx-IV variant custom-designed for production and secretion in human cells (ssHwTx) (Fig. 1). To confirm the biological activity of ssHwTx in vitro, we engineered a synthetic painkiller-screening assay in human embryonic kidney cells (HEK293) based on hNa_V1.7-dependent excitation–transcription coupling (designated as PainAssay) (Fig. 1, Supplementary Fig. 1a). In PainAssay, membrane depolarization activates hNa_V1.7 and subsequently triggers the opening of voltage-gated calcium channels, increase of cytosolic

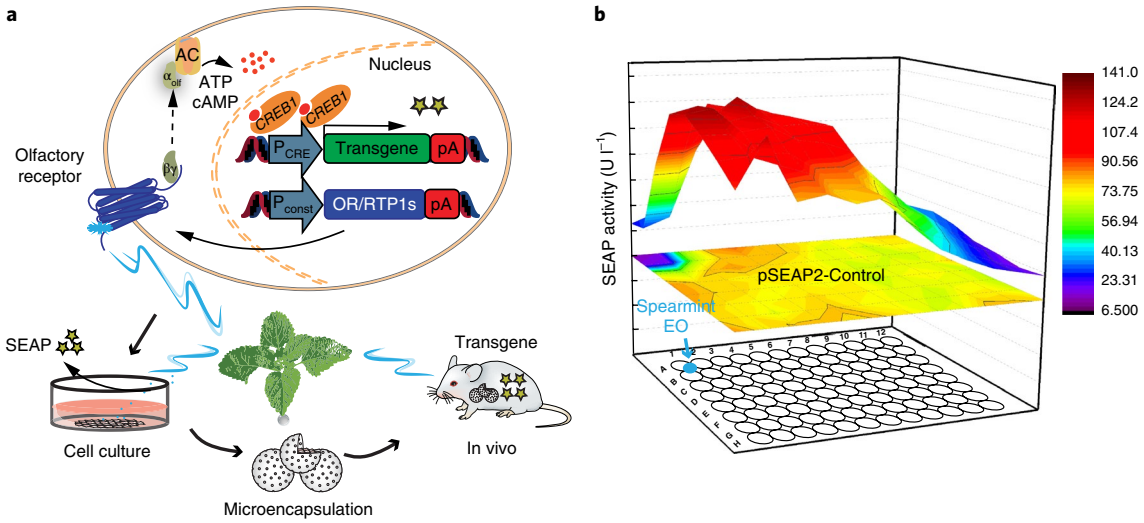

Fig. 3 | Engineering human cells for spearmint-inducible gene expression. a, Design principle. Ectopic expression of a R-carvone-specific mammalian olfactory receptor (OR) and the short version of the receptor-transporting protein 1 (RTP1s) in human cells enables spearmint-triggered olfactory neuron-specific G protein (G_{olf})-mediated activation of adenylate cyclase (AC), which converts adenosine triphosphate (ATP) into the second messenger, cAMP. The cAMP activates protein kinase A, resulting in phosphorylation and nuclear translocation of CREB1 and transcriptional activation of synthetic P_{CRE} promoters. Microencapsulated human cells transgenic for spearmint-triggered production and secretion of therapeutic transgene products could provide on-demand remote control of drug release in vivo following implantation. P_{const} denotes constitutive promoter. **b**, Distance-dependent SEAP expression (in units per litre). Hana3A cells were cotransfected with pWH13 ($P_{EF1\alpha}$-MOR256-17-pA), pRTP1s ($P_{EF1\alpha}$-RTP1s-pA) and pCK53 (P_{CRE}-SEAP-pA) and seeded into a 96-well tissue culture plate. Hana3A cells transfected with pSEAP2-Control (P_{SV40}-SEAP-pA) were used as cytotoxicity control. SEAP levels in culture supernatants were scored at 48 h after placing 150 µl of diluted spearmint essential oil (EO) (1:100, v/v) into an interwell cavity that had no physical contact with the cultivated cells. The heat map correlates numeric values for SEAP activity to a colour code that is used in the three-dimensional surface plot. All plasmids are described in Supplementary Table 1.

calcium and transsilencing of reporter gene expression driven by nuclear factor of activated T cells (NFAT) (Supplementary Fig. 1a). Inhibition of $Na_V1.7$ prevents depolarization-dependent gene transsilencing and results in increased reporter gene expression (Fig. 1). This modular architecture of PainAssay enables quantification of the effects of ectopically expressed $Na_V1.7$ on the cells' endogenous depolarization-dependent response of NFAT-responsive promoters (P_{NFAT}) (Supplementary Fig. 1b,c), and therefore the assay can be applied in vitro to validate compounds as potential $Na_V1.7$ channel modulators in the context of peripheral pain (Fig. 1).

When we examined analgesic compounds with PainAssay, only ssHwTx and the high-affinity $Na_V1.7$ blocker XEN907 ($IC_{50} \approx 3$ nM) (ref. [12]) could mediate dose-dependent expression of human placental secreted alkaline phosphatase (SEAP), while unspecific and low-affinity $Na_V1.7$ blockers such as amitriptyline ($IC_{50} \approx 1$ µM), tetracaine ($IC_{50} \approx 0.9$ µM) (ref. [13]) and lidocaine ($IC_{50} \approx 727$ µM) (ref. [14]), as well as negative control conditions such as dimethylsulfoxide and aspirin, did not substantially impact $Na_V1.7$ activity (Supplementary Fig. 1d–f). In particular, 0.35 µM ssHwTx achieved 49.3% ± 6.1% $Na_V1.7$ inhibition compared with the positive control (5 µM XEN907, taken as 100%) (Supplementary Fig. 1e). For precise quantification of $Na_V1.7$-dependent gene expression, intracellular green fluorescent protein (GFP) is more suitable than SEAP as it allows washing steps and medium exchange while retaining cellular memory over the entire experimental timespan. Indeed, when $hNa_V1.7$-transgenic HEK293 cells were resuspended in cell culture medium containing either XEN907 or ssHwTx, GFP expression levels confirmed the ability of ssHwTx to functionally inhibit $Na_V1.7$ in vitro (Fig. 2a).

To further validate effective and isoform-specific inhibition of $Na_V1.7$ by ssHwTx in vitro, we performed whole-cell patch clamp recordings confirming high affinity of ssHwTx for $Na_V1.7$ (Fig. 2b–d) and low affinity for the two most critical antitargets $Na_V1.5$ (Supplementary Fig. 2a,b) and voltage-gated potassium channel $K_V11.1$ (also known as the hERG protein) (Supplementary Fig. 2c,d). $Na_V1.5$ and $K_V11.1$ are predominantly expressed in the cardiac muscle, and their inhibition increases the risk for arrhythmia, stroke and sudden death[15]. Whole-cell voltage patch clamp of Chinese hamster ovary cells (CHO-K1) stably expressing $hNa_V1.7$ showed almost full inhibition of the channel's sodium current amplitudes in the presence of 450 nM ssHwTx (96.52% ± 2.24%) (Fig. 2b). Additional experiments confirmed that ssHwTx was a potent $Na_V1.7$ inhibitor across a wide ssHwTx concentration range (IC_{50} = 22.2 nM ± 1.3 nM) (Fig. 2c) and different depolarization shifts (Fig. 2d). In contrast, ssHwTx failed to inhibit $hNa_V1.5$ (Supplementary Fig. 2a,b) and human $K_V11.1$ (Supplementary Fig. 2c,d) even at higher levels of up to 1 µM.

Next, we evaluated the analgesic efficacy of ssHwTx in vivo using the formalin-induced mouse model of peripheral pain[16,17]. Following an intraplantar injection of formalin (5%, v/v in PBS buffer), the behavioural response of mice during the chronic pain phase (10–60 min after formalin injection) typically manifests in excessive licking and biting of the formalin-treated paw[18,19]. Mice implanted with microencapsulated ssHwTx-secreting HEK293 cells exhibited substantially reduced chronic pain behaviour compared with control mice treated with ssHwTx-deficient implants (Fig. 2e), although both implants showed equal protein production and secretion capacities (Fig. 2f). These results not only confirm the efficacy of ssHwTx in suppressing chronic pain[10], but also imply that high bioavailability can be achieved by using implanted human cells for in situ production and systemic delivery; the blood level of 3.61 nM ± 2.11 nM ssHwTx observed at 48 h after implantation afforded similar efficacy to that of HwTx-IV systemically injected at higher doses[10] (Fig. 2f). Importantly, ssHwTx did not appear to cause cardiovascular or behavioural side effects, as all mice retained normal blood pressure (Supplementary Fig. 2e) and normal locomotor functions (Supplementary Fig. 2f), while no serpentine tail movements or whole-body shaking were observed.

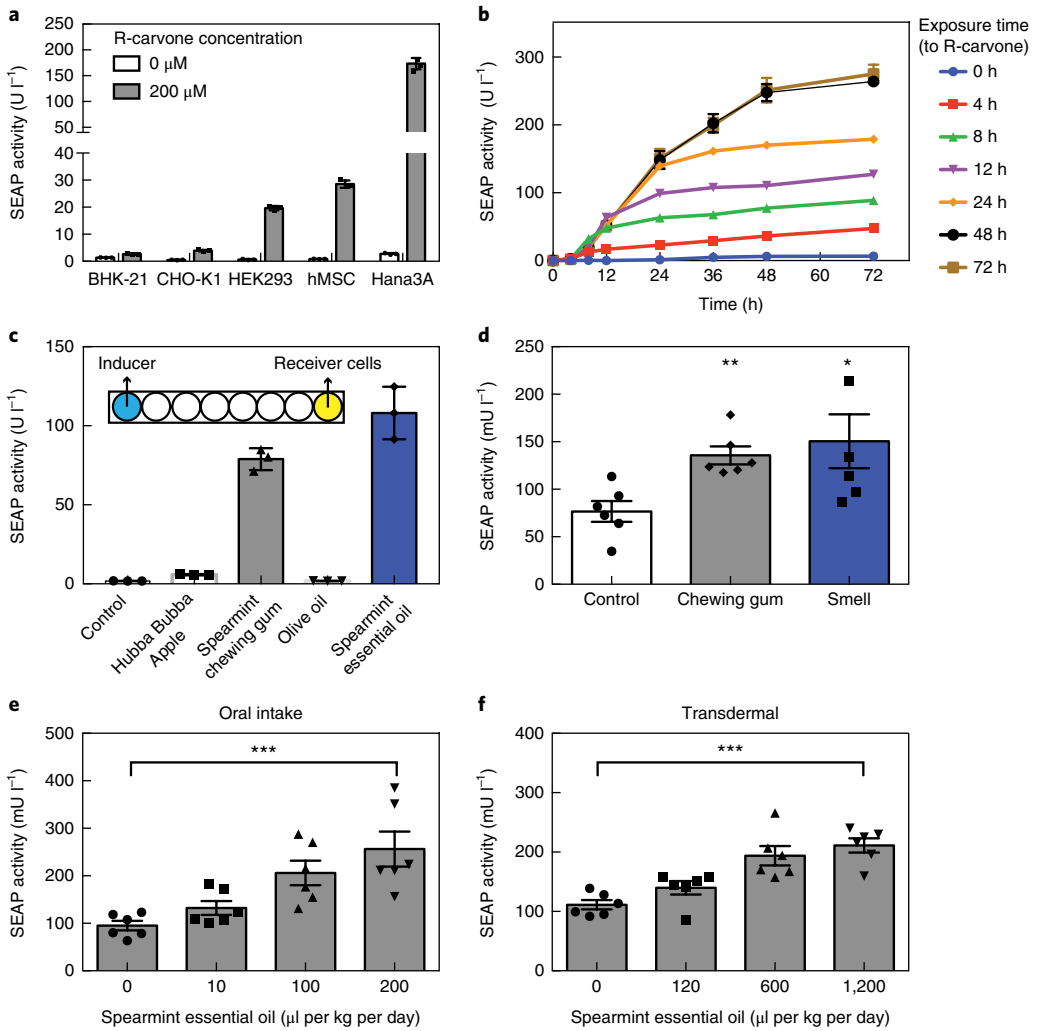

Fig. 4 | Validation of spearmint-inducible gene expression. a, R-carvone-triggered SEAP expression in mammalian cell lines. Baby hamster kidney cells (BHK-21), CHO-K1 cells, HEK293 cells, human mesenchymal stem cells (hMSC) and a HEK293-derived G_{olf}-transgenic Hana3A cell line were transfected with pWH13, pRTP1s and pCK53 and cultivated in culture medium containing 0 μM or 200 μM R-carvone for 48 h, then SEAP levels in the culture supernatants were scored. **b**, Hana3A cells were transfected with pWH13/pRTP1s/pCK53, stimulated with 200 μM R-carvone (time 0) for different durations and SEAP levels in culture supernatants were subsequently scored every 12 h. **c**, Control of SEAP expression with spearmint-containing food products. Hana3A cells were transfected with pWH13/pRTP1s/pCK53 and triggered by spearmint-containing chewing gum or essential oil placed in tissue culture wells that had no physical contact with the cultivated cells. SEAP levels in culture supernatants were scored at 48 h after stimulation. pWH13/pRTP1s/pCK53-transgenic cells cultivated in the absence of spearmint products were used as negative controls. Data in **a**–**c** are presented as mean ± s.d., $n = 3$ independent experiments. **d**–**f**, Spearmint-triggered SEAP expression in mice. pWH13/pRTP1s/pCK53-transgenic Hana3A cells were microencapsulated in alginate-poly-L-lysine-alginate beads and implanted into the intraperitoneal cavity (**d**,**e**) or subcutaneously into the lower dorsum (**f**) of mice. At 48 h after spearmint-based aromatherapy, SEAP levels in the animals' bloodstream were quantified. Data are shown as the mean ± s.e.m., statistics by two-tailed *t*-test (**d**) or one-way ANOVA test (**e**,**f**), $n = 6$ mice per group. $^*P < 0.05$, $^{**}P < 0.01$, $^{***}P < 0.001$ versus control. mU l^{-1}, milliunits per litre.

Programming human cells for spearmint-inducible transgene expression. To achieve remote-controlled transgene expression in human cells, we ectopically expressed an R-carvone-responsive murine olfactory receptor MOR256-17 derived from mammalian nose, and rewired its intracellular protein-kinase-A-dependent signalling cascade to cyclic adenosine monophosphate (cAMP)-mediated activation of synthetic cAMP-responsive promoter P_{CRE}-driven (where 'CRE' denotes cAMP-responsive element) SEAP expression[20] (Fig. 3a). R-carvone is a volatile compound that occurs naturally in *Mentha spicata* and accounts for the plant's characteristic spearmint odour. Indeed, when we characterized the R-carvone responsiveness in culture, distance-dependent SEAP activation could be triggered by a single drop of spearmint essential oil placed at a position on the tissue culture plate where it had no physical contact with the cultivated human cells (Fig. 3b). Control experiments revealed that SEAP expression could be dose-dependently tuned by adjusting the R-carvone concentration in the culture in the range of 0–200 μM, and importantly, a reporter-based cytotoxicity assay[21] confirmed that this R-carvone concentration range did not decrease the viability or overall protein secretion capacity of the cells (Supplementary Fig. 3a,b).

Among various mammalian cell lines tested, HEK293 and human mesenchymal stem cells showed optimal spearmint-triggered gene expression profiles (Fig. 4a). In particular, Hana3A cells, a HEK293-derived cell line stably expressing the olfactory neuron-specific G protein (G_{olf} protein), as well as receptor-transporting protein 1 (RTP1), receptor-transporting protein 2 and receptor expression-enhancing protein 1 chaperones that facilitate

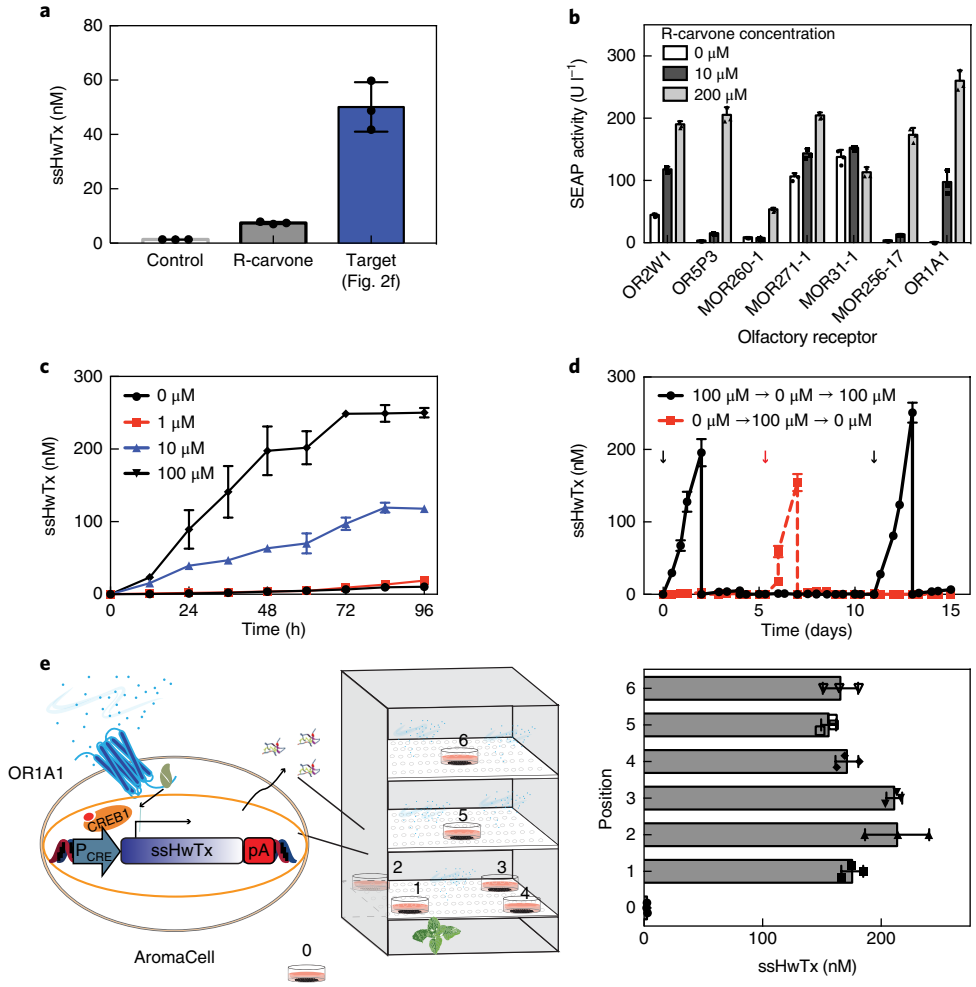

Fig. 5 | Construction and characterization of AromaCell line. a, Required profile for a spearmint-sensitive ssHwTx producer cell. To achieve effective pain suppression, human cells have to secrete ssHwTx at similar levels to those achieved with constitutive producer lines (see Fig. 2f) on stimulation with spearmint essential oil (10 μM). The genetic setup of pWH13/pRTP1s/pWH61-transgenic Hana3A cells fails to reach this target. **b**, Functional screening of different R-carvone-responsive olfactory receptors for spearmint-triggered SEAP expression. pRTP1s/pCK53-transgenic Hana3A cells were transfected with a pCI mammalian expression vector set (Promega) (pCI-OR2W1 (P_{hCMV}-CI-OR2W1-pA), pCI-OR5P3 (P_{hCMV}-CI-OR5P3-pA), pCI-MOR260-1 (P_{hCMV}-CI-MOR260-1-pA), pCI-MOR271-1 (P_{hCMV}-CI-MOR271-1-pA), pCI-MOR31-1 (P_{hCMV}-CI-MOR31-1-pA), pWH13 ($P_{EF\text{-}1\alpha}$-MOR256-17-pA) or pCI-OR1A1 (P_{hCMV}-CI-OR1A1-pA)) and cultivated for 48 h in cell culture medium containing different amounts of R-carvone, then the SEAP levels in the supernatants were scored. **c**–**e**, Characterization of AromaCells in vitro. **c**, ssHwTx-expression kinetics. AromaCells (4×10^5 cells per ml) were cultivated in R-carvone-free medium for 24 h, then different amounts of R-carvone were added and ssHwTx levels in culture supernatants were scored every 12 h. **d**, Reversibility. AromaCells (4×10^5 cells per ml) were cultivated for 15 days while R-carvone levels in the culture medium were successively switched between 0 and 100 μM. The cell density was readjusted to 4×10^5 cells per ml every 2–3 days. Cells were induced at 24 h after seeding (arrows), and cultured with R-carvone (100 μM) for 48 h. **e**, Spearmint-triggered remote control of ssHwTx production. AromaCell cultures were placed at different positions in an incubator (1–6) that was odourized with spearmint essential oil (100 μl per m^3). ssHwTx levels in the culture supernatants were scored after 48 h. All data are presented as mean ± s.d., $n = 3$ independent experiments. All plasmids are described in Supplementary Table 1.

G-protein-coupled receptor expression[22], showed the highest induction ratios between basal and spearmint-induced SEAP expression (Fig. 4a), as well as rapid and adjustable activation kinetics (Fig. 4b), and effective remote control by spearmint-containing food products (Fig. 4c, Supplementary Fig. 3c). Aromatherapy, the therapeutic use of essential oils extracted from plants through oral intake, topical application or inhalation, has been widely used to control a variety of persistent discomforts with high patient convenience[23]. Therefore, to test the compatibility of spearmint-regulated transgene expression with aromatherapy, we implanted mice with microencapsulated spearmint-triggered SEAP-expressing Hana3A cells (Fig. 3a, Supplementary Fig. 3d). After confirming that SEAP levels in the animals' bloodstream could be dose-dependently triggered by ingested R-carvone (Supplementary Fig. 3e), we allowed the mice to consume spearmint-flavoured chewing gum extract (Fig. 4d) or to inhale freely diffused spearmint essential oil (Fig. 4d), or we provided spearmint-containing olive oil either orally (Fig. 4e) or through transdermal delivery (Fig. 4f). In every case, exposed animals showed spearmint-dependent SEAP expression (Fig. 4d–f). However, the maximal induction fold between spearmint-activated and basal SEAP levels in vivo (Supplementary Fig. 3e) was markedly reduced when compared with that obtained in vitro (Supplementary Fig. 3d). Also, when we switched to an isogenic P_{CRE}-regulated ssHwTx-expression vector pWH61 (P_{CRE}-ssHwTx-pA) instead of pCK53 (P_{CRE}-SEAP-pA), we observed only relatively low spearmint-triggered ssHwTx induction fold in vitro (Fig. 5a), and the blood ssHwTx level was not significantly different from the control in vivo (Supplementary Fig. 3f) when the mice were exposed to the same regimens that triggered spearmint-dependent SEAP activation (Fig. 4e).

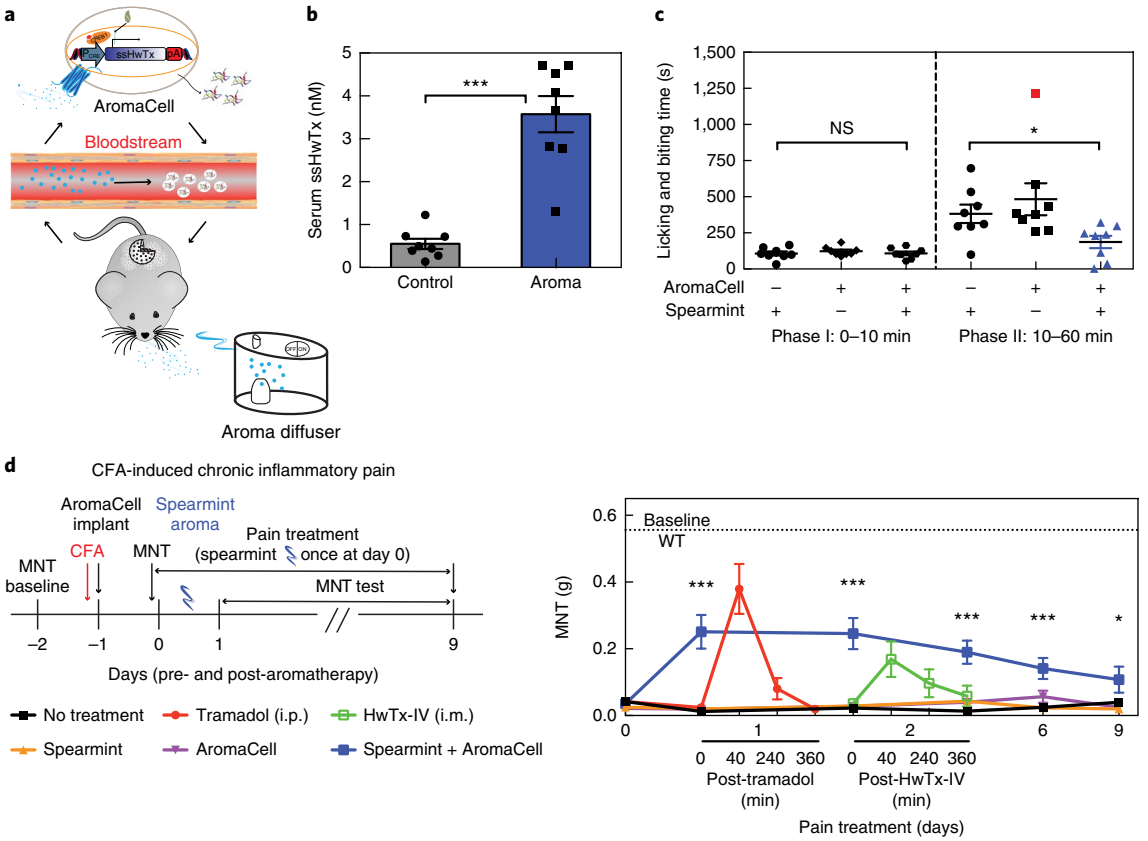

Fig. 6 | Validation of AromaCell-mediated pain therapy in mice. a, AromaCell-based therapeutic setting for treatment of chronic pain. Implantation of encapsulated AromaCells enables on-demand activation of ssHwTx release and pain suppression, remotely controlled with volatile spearmint aroma. **b**,**c**, Validation of AromaCell-mediated pain treatment potential by spearmint essential oil administration through an ultrasonic aroma diffuser; 6.5×10^6 microencapsulated AromaCells were implanted into mice. The mice were kept in spearmint essential-oil-odourized (using the aroma diffuser) rooms for 48 h, then ssHwTx levels in the bloodstream were scored (**b**) and formalin tests were performed to determine analgesic efficacy (**c**). Mice implanted with AromaCells but not exposed to spearmint or mice that did not receive AromaCells but were kept in the same spearmint-odourized room were used as negative controls. An outlier determined according to the ROUT method [44] is marked in red. **d**, AromaCell-mediated spearmint aromatherapy of chronic inflammatory pain. Left: experimental schedule. Right: pain treatment results. Chronic pain was induced by intraplantar injection of CFA, and pain sensation of mice was determined by profiling the MNT for two weeks. Treatment groups received either spearmint aromatherapy (3×10^6 microencapsulated AromaCells and 24 h administration of spearmint essential oil by aroma diffuser) or intraperitoneal (i.p.) injections of tramadol (50 mg per kg) or intramuscular (i.m.) injections of HwTx-IV (25 μg per kg). Mice implanted with AromaCell but not exposed to spearmint, or mice that did not receive AromaCells but were kept in the same spearmint-odourized room, were used as negative controls. The average MNT (0.56 ± 0.05 g, $n=50$ mice) of wild-type mice (WT) that did not receive CFA was set as the baseline for physiological pain sensation. Data of **b**–**d** are shown as the mean ± s.e.m., statistics by two-tailed *t*-test (**b**) and one-way ANOVA test (**c**,**d**), $n=8$ mice per group. $^*P<0.05$, $^{**}P<0.01$ versus control.

Design and characterization of the spearmint-sensitive AromaCell line. Therefore, it was necessary to increase the spearmint-dependent ssHwTx-productivity (Fig. 5a). For this purpose, we tested various mammalian R-carvone-responsive olfactory receptors and found that human OR1A1 (ref. [24]) afforded superior spearmint sensitivity and ssHwTx production capacity (Fig. 5b). We also reengineered the cAMP-responsive promoter P_{CRE} and found that the number of operator binding sites for human CRE binding protein 1 (CREB1) correlated with the spearmint-triggered production level (Supplementary Fig. 4a). We established that human elongation factor-1α promoter $P_{hEF\text{-}1\alpha}$-driven OR1A1 enabled optimal spearmint-dependent gene expression from a P_{CRE} promoter variant containing nine CREB1 binding sites (Supplementary Fig. 4a). Next, we stably integrated the corresponding genetic components into Hana3A cells. Among the 150 single cells randomly selected and clonally expanded from a triple-transgenic Hana3A population, cell clone number 93 fulfilled the requirements of a spearmint-sensitive ssHwTx-producing cell line (Supplementary Fig. 4b). It shows negligible basal ssHwTx secretion, produces ssHwTx in similar amounts to constitutively ssHwTx-expressing human cells when induced with low R-carvone concentrations (10 μM) and produced almost double the amount of ssHwTx when induced with 100 μM R-carvone (Supplementary Fig. 4b). Production of ssHwTx could be rapidly and precisely induced by adjusting the R-carvone concentration (Fig. 5c). A time-course experiment involving cycles of alternating R-carvone sensitization and desensitization confirmed that ssHwTx production could be programmed in a reversible manner (Fig. 5d). Thus, ssHwTx production in this cell line can be remotely controlled by the volatile component of spearmint essential oil (Fig. 5e). The spearmint-triggered ssHwTx production profile was reproducible for over 30 passages of the cell line (Supplementary Fig. 4c), which we designated as AromaCell.

Spearmint aromatherapy for AromaCell-mediated treatment of chronic pain. Inhalation is one of the most effective administration routes for essential oils, particularly when an ultrasonic aroma diffuser is employed[25,26] (Fig. 6a), and indeed, animal groups treated with the aroma diffuser showed the highest R-carvone

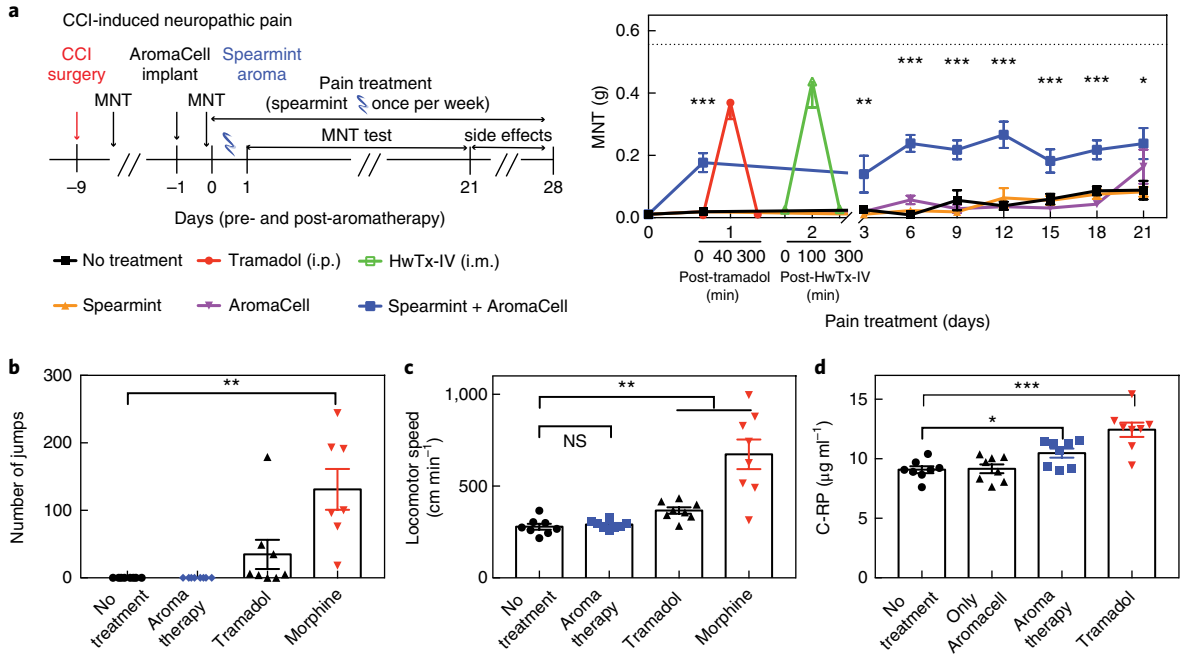

Fig. 7 | AromaCell-mediated pain therapy in CCI mice. a, AromaCell-mediated spearmint aromatherapy of chronic neuropathic pain. Left: experimental schedule. Right: pain treatment results. Chronic pain was induced by physical constriction of the left sciatic nerve of mice. Resulting mice with CCI were either treated with spearmint aromatherapy (3×10^6 microencapsulated AromaCells and weekly 24 h administration of spearmint essential oil) or received intraperitoneal injections of tramadol (50 mg per kg) or intramuscular injections of HwTx-IV (50 μg per kg). Pain sensation of treated and control mice were determined by scoring MNT for four weeks. **b**–**d**, Comparative assessment of side effects of pain treatment such as addiction (**b**), locomotor activity (**c**) and inflammation (**d**). **b**, Mice treated for three weeks with AromaCells as described in **a**, tramadol (3×50 mg per kg per day for 12 consecutive days) or morphine (3×50 mg per kg per day for three consecutive days) received one intraperitoneal injection of naloxone (4 mg per kg), and jumps representing drug withdrawal effects were counted for 30 min. **c**, Mice described in **b** were videorecorded, and the locomotor activity of each animal was analysed using the idTracker software [46]. **d**, After completing the chronic pain treatment described in **b**, serum C-reactive peptide (C-RP) levels were measured by enzyme-linked immunosorbent assay. Data of **a**–**d** are shown as the mean ± s.e.m., statistics by one-way ANOVA test (**a**) and two-tailed *t*-test (**b**–**d**), $n=8$ mice per group. $^*P<0.05$, $^{**}P<0.01$, $^{***}P<0.001$ versus control.

levels in blood, compared with other administration routes examined (Supplementary Fig. 5a). This suggested that a human lifestyle-compatible, aromatherapy-based pain treatment setting would be feasible. To test this idea, mice were implanted with a single dose of microencapsulated AromaCells (Supplementary Fig. 5b) and treated with spearmint essential oil either orally (Supplementary Fig. 5c,d) or via the aroma diffuser (Fig. 6b,c). Spearmint-mediated pain suppression was observed in both cases (Fig. 6c, Supplementary Fig. 5d,e, Supplementary Movie 1), but mice treated with the aroma diffuser showed higher spearmint-triggered ssHwTx levels in the bloodstream (Fig. 6b, Supplementary Fig. 5c). Control mice implanted with AromaCells but not exposed to spearmint essential oil, and mice that did not receive the therapeutic implant but were exposed only to spearmint, did not show any amelioration of the behavioural symptoms indicative of chronic pain (Fig. 6c, Supplementary Fig. 5d,e, Supplementary Movie 1). We confirmed that ssHwTx production could be repeatedly triggered with spearmint essential oil over the course of at least three weeks (Supplementary Fig. 5f). No immunogenicity was observed in the implanted mice over the same period (Supplementary Fig. 5g).

In addition to the validation of the therapy for persistent peripheral pain (Fig. 6a–c), we further confirmed the potential of AromaCell in two other chronic pain models simulating hyperalgesia resulting from chronic inflammations[27] (pain induced by complete Freund's adjuvant (CFA)) and neuropathic pain[16] (triggered by chronic constrictive injury (CCI)), the most refractory chronic pain condition. CFA mice treated with AromaCells and exposed for 24 h to spearmint essential oil atomized by an aroma diffuser showed sustained pain suppression for over nine days, whereas treatment groups receiving tramadol or native HwTx-IV were free of pain for up to only six hours (Fig. 6d). In contrast, oral intake of native HwTx-IV did not show any analgesic effect (Supplementary Fig. 6a). CCI mice treated with AromaCells and exposed once per week to spearmint essential oil atomized by an aroma diffuser were free of pain for the entire four-week experimental period, during which the spearmint-free treatment groups showed significant pain symptoms[28] (Fig. 7a).

Injection of HwTx-IV inhibited hyperalgesia (Fig. 7a), but only at excessive doses causing severe side effects such as torpidity, lethargy and death (Supplementary Fig. 6b). In contrast with conventional analgesics such as tramadol and morphine, prolonged treatment with AromaCell-secreted ssHwTx (Supplementary Fig. 6c) elicited neither drug tolerance (Fig. 7a) nor addiction (Fig. 7b). Additionally, whereas tramadol and morphine are also known to cause hyperactivity (Fig. 7c), Straub-tail reactions (Supplementary Movie 2) and seizures (Supplementary Movie 3), none of these behavioural side effects were observed for the spearmint-controlled ssHwTx-based AromaCell therapy (Fig. 7b,c, Supplementary Movie 4). Furthermore, compared with conventional pain treatment, AromaCells reduced the risk for inflammation (Fig. 7d), and treated animals did not show any significant changes in blood pressure (Supplementary Fig. 6d) and body weight (Supplementary Fig. 6e) that are typical for conventional small-molecule-based pain treatment.

Discussion

The clinical treatment of chronic pain remains problematic, and new strategies are required[5,29]. Convergent studies in the past decade have identified voltage-gated sodium channel $Na_V1.7$ (encoded by

the human *SCN9A* gene) as a prime molecular target for treatment of refractory chronic pain[4]. Humans lacking this channel are completely insensitive to pain[30], but retain proprioception, touch sensation, temperature discrimination, and normal motor functions[2,4]. Therefore, subtype-specific $Na_V1.7$-inhibitors such as HwTx-IV are considered promising candidates for potent and safe analgesics to treat chronic peripheral pain without the risk of side effects or addiction[4,8]. However, although HwTx-IV can be delivered systemically, poor bioavailability necessitates repeated injections to achieve sustained drug action[10], which can cause inflammation and tissue injury and impair quality of life. Focusing on the capacity of human cells to produce protein therapeutics with high efficiency and the availability of synthetic biology-inspired cell-engineering principles to construct custom-design human cells with novel functions[31], we constructed a monoclonal Hana3A cell line called AromaCell, which is stably transgenic for R-carvone-stimulated expression of the secretion-engineered and stabilized derivative of HwTx-IV (ssHwTx). Using AromaCell, ssHwTx production in mice could be precisely controlled by spearmint aromatherapy. Thus, by integrating recent breakthroughs in pain research, synthetic biology and aromatherapy, we have constructed a system that combines the non-invasive nature of spearmint aroma as a patient-convenient trigger compound, the versatility of engineered human cells in providing robust, tunable and on-demand ssHwTx secretion, and the high potency, safety and specificity of ssHwTx in treating chronic pain. We believe that this work provides a proof-of-concept cell-based therapy as a next-generation strategy to achieve robust, tunable, on-demand and side-effect-free analgesia for long-term management of chronic pain.

Currently, we engineered AromaCell using human cell lines and could validate its safety, toxicology and antinociceptive efficacy in animal models simulating all three chronic pain conditions in humans: persistent peripheral pain[16,17], neuropathic pain[16] and pain resulting from chronic inflammations[27]. Future clinical applications of AromaCell-based pain therapy may foresee night-time exposure of patients to spearmint essential oil vapourized by an ultrasonic aroma diffuser or inhalation of the spearmint aroma using modified electronic cigarettes providing portable, lifestyle-compatible and personalized treatment of pain flare-ups.

To translate this pain management strategy into a clinical reality, future work should focus on incorporating the functional components of AromaCell into clinically validated human cell types such as patient-derived autologous somatic cells or adipose-derived mesenchymal stem cells[32]. Although reimplantation of AromaCell-carrying autologous cells is not expected to cause immunogenic complications, a final therapy should still consist of encapsulated therapeutic cells inside a semipermeable and immunoisolating container, to enable flexible exchangeability of the implant in cases of dose renewal or fibrosis[33]. To this end, macroencapsulation architectures tailor-designed for subcutaneous implantation would be an optimal future implementation for AromaCell, which would combine easy surgical accessibility, patient compliance and effective vascularization, and might evolve as the therapy of choice for life-long management of chronic pain.

Methods

Vector design. Comprehensive design and construction details for all expression plasmids are provided in Supplementary Table 1. A Gly-Lys dipeptide motif was introduced at the C terminus of ssHwTx (hFc-HwTx-IV, where 'h' denotes human) to facilitate amidation by peptidylglycine α-amidating monooxygenase enzymes in vivo to afford the bioactive form of HwTx-IV (refs [34,35]).

Production of microcapsule implants. Cell implants were produced by microencapsulating transgenic HEK293, Hana3A or AromaCell (stably pWH113/pWH114/pWH117-transfected Hana3A) into coherent alginate-(poly-L-lysine)-alginate capsules (400 µm, 200 cells per capsule) using an Inotech Encapsulator Research IE-50R (EncapBioSystems) with the following parameters: a 200 µm nozzle with a vibration frequency of 1,025 Hz, a 25 mL syringe operated at a flow rate of 410 units, and 1.12 kV voltage for bead dispersion[36]. Capsule integrity was confirmed by microscopy, and functionality was confirmed by analytical assays in vitro before injecting 10,000–50,000 capsules (200 cells per capsule) into the intraperitoneal cavity or into the lower dorsum subcutaneously of mice.

Spearmint aromatherapy in mice. Adult OF1 mice (female, 7–8 weeks; Charles River), CD-1 Swiss mice (male, 8–12 weeks; Charles River) or C57BL/6J mice (female, 8–12 weeks; East China Normal University) were acclimatized to the environment for at least 7 days before the start of all studies. Mice harbouring microcapsule implants received R-carvone through oral intake of R-carvone (0–200 mg per kg per day, three times every 24 h, diluted in 600 µl olive oil), oral intake of spearmint essential oil (0–500 µl per kg per day, three to six times every 24 h, diluted in 600 µl olive oil), oral intake of spearmint chewing gum extract solution (1,200 µl per mouse per day, four times every 24 h), topical application (0–1,200 µl per mouse per day, three times every 24 h to shaved skin, diluted in 600 µl olive oil), or inhalation of spearmint essential oil by natural volatilization, by application of R-carvone to the nasal mucous membrane (20 µl of 20 mM stock solution per mouse, six times every 24 h) or by dispensing spearmint essential oil with a Bel-Air ultrasonic aroma diffuser (Welfine). The aroma diffuser was placed into a 60 cm × 40 cm chamber harbouring the cage containing the mice, and pure spearmint essential oil was dispersed by ultrasonic atomization on a rhythm of 5 s on and 10 s off over 24 h or 48 h. During all experiments, animals had free access to water and food. Following spearmint treatment, mice were analysed for different behaviours or for transgene expression by collecting blood samples using Microtainer serum separating tubes (BD, catalogue no. 365967).

Formalin-induced persistent pain. The formalin-based mouse model encompasses inflammatory, neurogenic and central mechanisms of nociception[18,19]. Briefly, after acclimatization to the experimental environment for one week, CD-1 Swiss mice were injected with 20 µl of 5% buffered formalin solution on the plantar surface of a hind paw using 30G Hamilton syringes (catalogue no. HA-80508-13) and counting the animals' total licking and biting time of the formalin-treated paw over the course of 60 min (phase I, acute pain behaviour, 0–10 min; phase II, chronic pain behaviour, 10–60 min). During the formalin test, all animals were kept in individual polycarbonate chambers set up with back and bottom mirrors, and the entire experiment (from 10 min before formalin injection to the completion of the formalin test) was video-captured with an iPad (front view) and iPhone (top view).

Measurement of mechanical nociceptive threshold (MNT). Chronic hyperalgesia of mice was determined by measuring the exaggerated nocifensive response of a paw towards a mechanical stimulus. Mechanosensitivity was measured according to a simplified up–down method[37] using nine von Frey filaments (Ugo Basile) spanning forces ranging from 0.008 g to 1.4 g (refs [38,39]). Mice were placed in polycarbonate chambers on an elevated mesh floor, acclimatized for at least 20 min to the testing environment, and the MNT was measured by pressing the von Frey fibres against the mid-plantar surface of the hind paw for a total of five times. The fibre was held slightly buckled for 5–8 s with an interstimulus interval of at least 10 s (ref. [40]). Withdrawal, flinching, biting and licking of the stimulated paw were recorded as positive responses. The MNT value was calculated using the formula: MNT = force of fifth fibre applied ± 0.5 × last stimulus interval (ref. [39]). Measurement of a MNT-series was always performed by a same investigator who was blinded to the treatment condition of an individual animal.

Mouse model of CFA-induced chronic inflammatory pain. To induce chronic inflammatory pain, 20 µl of freshly emulsified CFA (1 : 1, v/v in sterile PBS) was injected subcutaneously into the plantar surface of the left hind paw of C57BL/6J mice using 30 G Hamilton syringes. Chronic pain typically develops 24 h after CFA administration[27,41,42]. Hyperalgesia of mice was determined by the MNT values obtained from mechanical stimulation using von Frey fibres.

Mouse model of CCI-induced chronic neuropathic pain. C57BL/6J mice with CCI were purchased from ChemPartner. The surgery procedure was performed as described by Bennett and Xie[43] with minor adaptation for mice. Under anaesthesia, the left sciatic nerve of mice was loosely tied with three ligatures of 6-0 silk sutures at 1 mm intervals. Hyperalgesia and allodynia were confirmed by measuring MNT values using von Frey fibres.

Ethics. Animal experiments were performed according to the directive of the European Community Council (2010/63/EU), approved by the French Republic (project nos DR2014-42 and DR2016-13), and carried out by G.C. (grant no. 69266309) and M. Daoud-El Baba (grant no. 69266310) at the University Institute of Technology of the University of Lyon (F-69622 Villeurbanne). Animal experiments related to Figs. 6d and 7a,d and Supplementary Fig. 6a–c were performed in the laboratory of H.Y. according to the protocol (m20170803) approved by the East China Normal University Animal Care and Use Committee and in direct accordance with the Ministry of Science and Technology of China on Animal Care Guidelines.

Data analysis. Relative inhibition (%) of hNa$_V$1.7 by ssHwTx was calculated as [(SEAP value by 0.35 µM ssHwTx / baseline SEAP for ssHwTx) − 1] / [(SEAP value by 5 µM XEN907 / SEAP value by dimethylsulfoxide) − 1] × 100. All values for in vitro experiments represent the mean ± standard deviation (s.d.) of independent experiments. For in vivo experiments, all values are expressed as the mean ± standard error of the mean (s.e.m.). Each mice group was randomly selected from the same delivered pool with the particular genetic background. Outlier tests were performed according to the robust regression and outlier removal (ROUT) method[44]. After assessing normality assumptions and group standard deviations, data of experiments comparing two test groups were analysed with an unpaired Welch's *t*-test, which excludes the assumption of equal variances. For experiments comparing more than two test groups, data were analysed using one-way analysis of variance (ANOVA). All analyses were performed using Prism 7 software (GraphPad).

Life Sciences Reporting Summary. Further information on experimental design is available in the Life Sciences Reporting Summary.

Data availability. The data that support the findings of this study are available within the paper and its Supplementary Information.

Received: 9 May 2017; Accepted: 9 January 2018;
Published online: 6 February 2018

References

1. Lampert, A., O'Reilly, A. O., Reeh, P. & Leffler, A. Sodium channelopathies and pain. *Pflug. Arch. Eur. J. Phy.* **460**, 249–263 (2010).
2. King, G. F. & Vetter, I. No gain, no pain: Na$_V$1.7 as an analgesic target. *ACS Chem. Neurosci.* **5**, 749–751 (2014).
3. Goins, W. F., Cohen, J. B. & Glorioso, J. C. Gene therapy for the treatment of chronic peripheral nervous system pain. *Neurobiol. Dis.* **48**, 255–270 (2012).
4. Dib-Hajj, S. D., Yang, Y., Black, J. A. & Waxman, S. G. The Na$_V$1.7 sodium channel: from molecule to man. *Nat. Rev. Neurosci.* **14**, 49–62 (2013).
5. Grosser, T., Woolf, C. J. & FitzGerald, G. A. Time for nonaddictive relief of pain. *Science* **355**, 1026–1027 (2017).
6. Adams, D. J., Callaghan, B. & Berecki, G. Analgesic conotoxins: block and G protein-coupled receptor modulation of N-type (Ca$_V$2.2) calcium channels. *Br. J. Pharmacol.* **166**, 486–500 (2012).
7. McGivern, J. G. Ziconotide: a review of its pharmacology and use in the treatment of pain. *Neuropsychiatr. Dis. Treat.* **3**, 69–85 (2007).
8. Revell, J. D. et al. Potency optimization of Huwentoxin-IV on *h*Na$_v$1.7: a neurotoxin TTX-S sodium-channel antagonist from the venom of the Chinese bird-eating spider *Selenocosmia huwena*. *Peptides* **44**, 40–46 (2013).
9. Murray, J. K. et al. Engineering potent and selective analogues of GpTx-1, a tarantula venom peptide antagonist of the Na$_V$1.7 sodium channel. *J. Med. Chem.* **58**, 2299–2314 (2015).
10. Liu, Y. et al. Analgesic effects of Huwentoxin-IV on animal models of inflammatory and neuropathic pain. *Protein Pept. Lett.* **21**, 153–158 (2014).
11. Ye, H. et al. Self-adjusting synthetic gene circuit for correcting insulin resistance. *Nat. Biomed. Eng.* **1**, 1–9 (2016).
12. Chowdhury, S. et al. Discovery of XEN907, a spirooxindole blocker of Na$_V$1.7 for the treatment of pain. *Bioorg. Med. Chem. Lett.* **21**, 3676–3681 (2011).
13. McCormack, K. et al. Voltage sensor interaction site for selective small molecule inhibitors of voltage-gated sodium channels. *Proc. Natl Acad. Sci. USA* **110**, E2724–E2732 (2013).
14. Sheets, P. L., Jarecki, B. W. & Cummins, T. R. Lidocaine reduces the transition to slow inactivation in Na$_v$1.7 voltage-gated sodium channels. *Br. J. Pharmacol.* **164**, 719–730 (2011).
15. Gintant, G., Sager, P. T. & Stockbridge, N. Evolution of strategies to improve preclinical cardiac safety testing. *Nat. Rev. Drug Discov.* **15**, 457–471 (2016).
16. Lee, J. H. et al. A monoclonal antibody that targets a Na$_V$1.7 channel voltage sensor for pain and itch relief. *Cell* **157**, 1393–1404 (2014).
17. Vissers, K. C., Geenen, F., Biermans, R. & Meert, T. F. Pharmacological correlation between the formalin test and the neuropathic pain behavior in different species with chronic constriction injury. *Pharmacol. Biochem Behav.* **84**, 479–486 (2006).
18. Hunskaar, S., Fasmer, O. B. & Hole, K. Formalin test in mice, a useful technique for evaluating mild analgesics. *J. Neurosci. Methods* **14**, 69–76 (1985).
19. Sufka, K. J., Watson, G. S., Nothdurft, R. E. & Mogil, J. S. Scoring the mouse formalin test: validation study. *Eur. J. Pain.* **2**, 351–358 (1998).
20. Dahoun, T., Grasso, L., Vogel, H. & Pick, H. Recombinant expression and functional characterization of mouse olfactory receptor mOR256-17 in mammalian cells. *Biochemistry* **50**, 7228–7235 (2011).
21. Sun, N., Lee, A. & Wu, J. C. Long term non-invasive imaging of embryonic stem cells using reporter genes. *Nat. Protoc.* **4**, 1192–1201 (2009).
22. Saito, H., Kubota, M., Roberts, R. W., Chi, Q. & Matsunami, H. RTP family members induce functional expression of mammalian odorant receptors. *Cell* **119**, 679–691 (2004).
23. Reichling, J., Schnitzler, P., Suschke, U. & Saller, R. Essential oils of aromatic plants with antibacterial, antifungal, antiviral, and cytotoxic properties—an overview. *Forsch. Komplementmed.* **16**, 79–90 (2009).
24. Muller, M. et al. Designed cell consortia as fragrance-programmable analog-to-digital converters. *Nat. Chem. Biol.* **13**, 309–316 (2017).
25. Ni, C. H. et al. The anxiolytic effect of aromatherapy on patients awaiting ambulatory surgery: a randomized controlled trial. *Evid. Based Compl. Alt.* **2013**, 927419 (2013).
26. Bilia, A. R. et al. Essential oils loaded in nanosystems: a developing strategy for a successful therapeutic approach. *Evid. Based Compl. Alt.* **2014**, 651593 (2014).
27. Xu, Z. Z. et al. Resolvins RvE1 and RvD1 attenuate inflammatory pain via central and peripheral actions. *Nat. Med.* **16**, 592–597 (2010).
28. Liu, C., Cao, J., Ren, X. & Zang, W. Na$_v$1.7 protein and mRNA expression in the dorsal root ganglia of rats with chronic neuropathic pain. *Neural Regen. Res.* **7**, 1540–1544 (2012).
29. Burgess, G. & Williams, D. The discovery and development of analgesics: new mechanisms, new modalities. *J. Clin. Investig.* **120**, 3753–3759 (2010).
30. Cox, J. J. et al. An SCN9A channelopathy causes congenital inability to experience pain. *Nature* **444**, 894–898 (2006).
31. Xie, M. & Fussenegger, M. Mammalian designer cells: engineering principles and biomedical applications. *Biotechnol. J.* **10**, 1005–1018 (2015).
32. Trounson, A. & DeWitt, N. D. Pluripotent stem cells progressing to the clinic. *Nat. Rev. Mol. Cell Biol.* **17**, 194–200 (2016).
33. Lathuiliere, A., Cosson, S., Lutolf, M. P., Schneider, B. L. & Aebischer, P. A high-capacity cell macroencapsulation system supporting the long-term survival of genetically engineered allogeneic cells. *Biomaterials* **35**, 779–791 (2014).
34. Prohaska, J. R. & Broderius, M. Plasma peptidylglycine alpha-amidating monooxygenase (PAM) and ceruloplasmin are affected by age and copper status in rats and mice. *Comp. Biochem. Phys. B* **143**, 360–366 (2006).
35. Merkler, D. J. C-terminal amidated peptides: production by the in vitro enzymatic amidation of glycine-extended peptides and the importance of the amide to bioactivity. *Enzym. Microb. Technol.* **16**, 450–456 (1994).
36. Xie, M. et al. beta-cell-mimetic designer cells provide closed-loop glycemic control. *Science* **354**, 1296–1301 (2016).
37. Bonin, R. P., Bories, C. & De Koninck, Y. A simplified up-down method (SUDO) for measuring mechanical nociception in rodents using von Frey filaments. *Mol. Pain.* **10**, 26 (2014).
38. Denk, F., Crow, M., Didangelos, A., Lopes, D. M. & McMahon, S. B. Persistent alterations in microglial enhancers in a model of chronic pain. *Cell Rep.* **15**, 1771–1781 (2016).
39. Hassan, A. M. et al. Visceral hyperalgesia caused by peptide YY deletion and Y2 receptor antagonism. *Sci. Rep.* **7**, 40968 (2017).
40. Chaplan, S. R., Bach, F. W., Pogrel, J. W., Chung, J. M. & Yaksh, T. L. Quantitative assessment of tactile allodynia in the rat paw. *J. Neurosci. Methods* **53**, 55–63 (1994).
41. Ren, K. & Dubner, R. Inflammatory models of pain and hyperalgesia. *ILAR J.* **40**, 111–118 (1999).
42. Beko, K. et al. Contribution of platelet P2Y12 receptors to chronic Complete Freund's adjuvant-induced inflammatory pain. *J. Thromb. Haemost.* **15**, 1223–1235 (2017).
43. Bennett, G. J. & Xie, Y. K. A peripheral mononeuropathy in rat that produces disorders of pain sensation like those seen in man. *Pain* **33**, 87–107 (1988).
44. Motulsky, H. J. & Brown, R. E. Detecting outliers when fitting data with nonlinear regression—a new method based on robust nonlinear regression and the false discovery rate. *BMC Bioinformatics* **7**, 123 (2006).
45. Wang, H., Ye, H., Xie, M., Daoud El-Baba, M. & Fussenegger, M. Cosmetics-triggered percutaneous remote control of transgene expression in mice. *Nucleic Acids Res.* **43**, e91 (2015).
46 Branson, K. Distinguishing seemingly indistinguishable animals with computer vision. *Nat. Methods* **11**, 721–722 (2014).

Acknowledgements

We thank L. Scheller for critical comments on the manuscript; A. W. Xie (Welfine Science & Technology) for providing the Bel-Air aroma diffuser; V. Jäggin and T. Lopes for assistance with fluorescence-activated cell sorting; M. Daoud-El Baba, S. Xue and

J. Yin for help with animal experiments, and Y. Huang (ChemPartner) for the CCI-based mouse model; D. Bodenham for support with statistical analysis; and M. Müller, P. Saxena and R. Kojima for generous advice. This work was supported by a European Research Council advanced grant (ProNet, no. 321381), by the National Centre of Competence in Research Molecular Systems Engineering, the National Natural Science Foundation of China (grant nos 31522017, 31470834 and 31670869) and the Thousand Youth Talents Plan of China.

Author contributions

H.W., M.X., G.C.-E.H. and H.Y. conducted the experiments, and H.W., M.X. and M.F. designed the experiments and wrote the manuscript.

Competing interests

The authors declare no competing financial interests.

Additional information

Supplementary information is available for this paper at https://doi.org/10.1038/s41551-018-0192-3.

Reprints and permissions information is available at www.nature.com/reprints.

Correspondence and requests for materials should be addressed to M.F.

Publisher's note: Springer Nature remains neutral with regard to jurisdictional claims in published maps and institutional affiliations.

nature research

Corresponding author(s): Martin Fussenegger

Life Sciences Reporting Summary

Nature Research wishes to improve the reproducibility of the work that we publish. This form is intended for publication with all accepted life science papers and provides structure for consistency and transparency in reporting. Every life science submission will use this form; some list items might not apply to an individual manuscript, but all fields must be completed for clarity.

For further information on the points included in this form, see Reporting Life Sciences Research. For further information on Nature Research policies, including our data availability policy, see Authors & Referees and the Editorial Policy Checklist.

Please do not complete any field with "not applicable" or n/a. Refer to the help text for what text to use if an item is not relevant to your study.
For final submission: please carefully check your responses for accuracy; you will not be able to make changes later.

Experimental design

1. Sample size

Describe how sample size was determined.

Conventional methods: minimal 3 independent experiments per data point for in vitro studies and minimal 5 mice per treatment group for in vivo studies. Sample size determination as described in Stanley et al. Nat. Med. 21, 92 (2015).

2. Data exclusions

Describe any data exclusions.

Only outliers were excluded, according to the ROUT method [Motulsky H. J. et al. BMC 7, 123 (2006)]. Excluded outliers were marked in the respective figures (Fig. 4c).

3. Replication

Describe the measures taken to verify the reproducibility of the experimental findings.

All attempts at replication were successful.

4. Randomization

Describe how samples/organisms/participants were allocated into experimental groups.

Mice of the same genetic background were randomly distributed into different experimental groups.

5. Blinding

Describe whether the investigators were blinded to group allocation during data collection and/or analysis.

All investigators during data analysis were blinded to the treatment condition.

Note: all in vivo studies must report how sample size was determined and whether blinding and randomization were used.

6. Statistical parameters

For all figures and tables that use statistical methods, confirm that the following items are present in relevant figure legends (or in the Methods section if additional space is needed).

n/a	Confirmed
☐	☒ The exact sample size (*n*) for each experimental group/condition, given as a discrete number and unit of measurement (animals, litters, cultures, etc.)
☐	☒ A description of how samples were collected, noting whether measurements were taken from distinct samples or whether the same sample was measured repeatedly
☐	☒ A statement indicating how many times each experiment was replicated
☐	☒ The statistical test(s) used and whether they are one- or two-sided *Only common tests should be described solely by name; describe more complex techniques in the Methods section.*
☐	☒ A description of any assumptions or corrections, such as an adjustment for multiple comparisons
☐	☒ Test values indicating whether an effect is present *Provide confidence intervals or give results of significance tests (e.g. P values) as exact values whenever appropriate and with effect sizes noted.*
☐	☒ A clear description of statistics including central tendency (e.g. median, mean) and variation (e.g. standard deviation, interquartile range)
☐	☒ Clearly defined error bars in all relevant figure captions (with explicit mention of central tendency and variation)

See the web collection on statistics for biologists for further resources and guidance.

Software

Policy information about availability of computer code

7. Software

Describe the software used to analyze the data in this study.	Graphpad Prism 7.

For manuscripts utilizing custom algorithms or software that are central to the paper but not yet described in the published literature, software must be made available to editors and reviewers upon request. We strongly encourage code deposition in a community repository (e.g. GitHub). *Nature Methods* guidance for providing algorithms and software for publication provides further information on this topic.

Materials and reagents

Policy information about availability of materials

8. Materials availability

Indicate whether there are restrictions on availability of unique materials or if these materials are only available for distribution by a third party.	All unique materials are readily available from the authors.

9. Antibodies

Describe the antibodies used and how they were validated for use in the system under study (i.e. assay and species).	We provided catalogue numbers and/or lot numbers for all antibodies and ELISA kits used in the study (see Methods and Supplementary Information).

10. Eukaryotic cell lines

a. State the source of each eukaryotic cell line used.	We have specified the source of the cell lines. See Methods and 'Cell culture and transfection' in the Supplementary Information.
b. Describe the method of cell line authentication used.	The Hana3A cell line is authenticated by the Matsunami group [Saito et al. Cell 119, 679-691 (2004)], and all the others were authenticated by ATCC. Stable cell lines developed in this work were authenticated by functionality tests, and are available upon request.
c. Report whether the cell lines were tested for mycoplasma contamination.	We exclusively use reference source material, which we regularly check for mycoplasma and other bacterial contaminations.
d. If any of the cell lines used are listed in the database of commonly misidentified cell lines maintained by ICLAC, provide a scientific rationale for their use.	No commonly misidentified cell lines were used.

Animals and human research participants

Policy information about studies involving animals; when reporting animal research, follow the ARRIVE guidelines

11. Description of research animals

Provide all relevant details on animals and/or animal-derived materials used in the study.	Adult OF1 mice (female, 7–8 weeks; Charles River Laboratories), CD-1 Swiss mice (male, 8–12 weeks; Charles River Laboratories) and C57BL/6J mice (female, 8–12 weeks; East China Normal University Laboratory Animal Center).

Policy information about studies involving human research participants

12. Description of human research participants

Describe the covariate-relevant population characteristics of the human research participants.	The study did not involve human research participants.